

Cantenna Adjustment with 1×6 Woodpile Shaped EBG for Application in Goat Manure Moisture Content and Bulk Density Monitoring

Watcharaphon Naktong¹, Sawitree Prapakarn²,
Natthapong Prapakarn³, and Natchayathorn Wattikornsirikul^{4,*}

Abstract—This study aimed to investigate the structural design of a cantenna with Woodpile shaped electromagnetic band gap (EBG) for gain enhancement and to increase the efficiency of signal transmission for measuring the moisture content and the bulk density of goat manure, which can help farmers reduce the cost of buying chemical fertilizers. From the test of operating frequency ranges from 2 to 3 GHz, it was found that the frequency band that responds to humidity the best is 2.60 GHz, increasing the efficiency of the gain with the $6 \times 6 \text{ cm}^2$ Woodpile shaped EBG. It was arranged in transverse electric (TE) and placed parallel to the end of the cantenna. This allows the gain to be increased to 9.31 dBi, in which the cantenna structure without EBG has the gain of 7.32 dBi. When the cantenna is used to determine the moisture content (MC) and bulk density, the transmission distance between the cantenna Tx/Rx is 3 cm with an average power rating of 0.0001–0.5 mW. This cantenna can measure humidity in the unit of wet basis (wb.) as low as 0.14%wb., at an average power of 0.5 mW.

1. INTRODUCTION

Nowadays, goat manure compost is very popular in Thailand because of its nutrients and microorganisms which are very beneficial for plants. The total nutrient content is nitrogen (N) 1.03, phosphorus (P) 0.66, and potassium (K) 0.64. Nitrogen is responsible for nourishing leaves, stems, and young shoots. Phosphorus nourishes flowers, fruits, seeds, as well as the color and sweetness of the fruit. Potassium nourishes root, system, and tubers. Goat manure is beneficial in that it dissolves slowly, giving the plants time to absorb the fertilizer, helping to loosen soil easily and is safe from chemicals, thus environmentally friendly. Goats are advantageous because of a shorter raising period than cows and have good tolerance to all weather conditions. They produce milk, meat, leather, or fur. Raising goats is very easy as they are small and easy to manage, take up less space, and there are many species to choose from. From the foregoing, a group of researchers has developed goat manure to be more efficient and more effective [1–5]. Nonetheless, there are still problems in measuring the moisture content and bulk density of goat manure, which both must be of appropriate values for the efficient use in growing plants. Based on such problems, some companies have built ultrasonic moisture meters with an operating frequency range of 20 kHz–1 GHz. The principle of transmitting frequency waves to material is used to measure moisture content and then reflect the wave back to the receiver. This can measure volumes up to 200 g.

Received 28 August 2022, Accepted 14 October 2022, Scheduled 31 October 2022

* Corresponding author: Natchayathorn Wattikornsirikul (natchayathorn.w@rmutp.ac.th).

¹ Department of Telecommunications Engineering, Faculty of Engineering and Technology, Rajamangala University of Technology Isan, Nakhon Ratchasima 30000, Thailand. ² Department of Agricultural Machinery Engineering, Faculty of Engineering and Technology, Rajamangala University of Technology Isan, Nakhon Ratchasima 30000, Thailand. ³ Department of Smart Farm Engineering, Institute of Interdisciplinary Studies, Rajamangala University of Technology Isan, Nakhon Ratchasima 30000, Thailand.

⁴ Department of Electronics and Telecommunications Engineering, Faculty of Engineering, Rajamangala University of Technology Phra Nakhon, Bangkok 10300, Thailand.

For example, the Halogen Moisture Analyzer HX204 and moisture analyzers are expensive due to their operating frequency range greater than 1 GHz. That can measure results as desired. Such tools are still expensive and take a long time to maintain because the equipment must be imported from abroad. Therefore, this study designs a device to measure the moisture content and bulk density (key factors) of goat manure compost with high-frequency waves or dielectric measurement through the antenna equipment [6–8]. The device was used as a transceiver which used electromagnetic band gap (EBG) technique to optimize the amplification of the wave power. The study was based on the research on waveguide antenna structure and microstrip antenna in combination with EBG as demonstrated in the literature review below.

A waveguide antenna structure using a rectangular horn antenna with two side-wing slabs for the use in radar systems in the X-band and Ku-band areas had a gain of 18.08 dB. When being combined with a wire EBG in a cosine arrangement at a distance of $(16.5\lambda) = 49.5$ cm from the antenna, it had a gain of 25.6 dB using the 10 GHz frequency range [9]. Another study explored a horn waveguide antenna using an asymmetric horn stub added for secondary radar system. It was used in combination with a rectangular EBG. It was arranged in a woodpile EBG hybrid metamaterial structure at a distance of 4.77 cm from the antenna with a size of 40×40 cm². The device operated in the 1.03 GHz, 1.09 GHz, and 1.30 GHz frequencies, with gain values ranging from 15.43 dB, 15.61 dB, and 14.46 dB, respectively [10]. A horn antenna had a bed of nails with a gain of 9.60 dBi for use in the Ku-Band radar system. This type of antenna used the technique of adding a rectangular stub. The side-lobe-level (SLL) layout was 0.45×0.3 cm², and it operated in the frequency range of 12.8–18 GHz with an average gain of 13.10 dBi [11]. A horn antenna excited by substrate-integrated gap waveguide for the use in Ku-band radar was combined with a mushroom EBG operating in the frequency range from 28.5–35 GHz and had an average gain 11.5 dBi [12]. A dual-polarization-switching cantenna used for wireless power transmitter for LED accessories operating in a 2.45 GHz frequency range had an average gain of 12.2 dBi [13]. A conventional circular horn antenna used for X-band radar and I-band beyond the IEEE and ITU in combination with a woodpile EBG structure operating in a frequency range of 10 GHz had an average gain of 25.34 dB [14]. A conventional circular horn antenna with a gain of 18.1 dB was used for C-band radar. When being combined with a planar mushroom EBG type conventional circular horn operating in a frequency range from 5 GHz, it had an average gain of 19.7 dB [15]. Another conventional circular horn antenna with a gain of 17.7 dB was used for X-band radar in combination with a double-wire EBG type conventional circular horn. This antenna operated in a frequency range of 10 GHz and had average gain 20.9 dB [16]. A conical horn antenna used for Ku-band radar using Gauss Process (GP) technique with coarse mesh in a frequency range of 10 GHz had an average gain of 12.76 dB [17]. A conventional circular horn antenna with a gain of 18.6 dB was used in the X-band Very Small Aperture Terminal (VSAT). The geometry of the axially corrugated conical horn antenna was used together with a double-layer medium wire type and a conventional circular horn grooving technique operating in the frequency range of 10.7 GHz to 14.5 GHz. The 12.75 GHz and 13.75 GHz frequencies had average gains of 38 dBi and 42 dBi, respectively [18]. A Fabry-Perot horn antenna, with a gain of 2.02 dBi, was applied to the X-band Very Small Aperture Terminal (VSAT) in combination with a Frequency Selective Surface (FSS) EBG type Frequency Selective Surface (FSS) grid dimensions serving as Partially Reflecting Surface (PRS) which operated in the frequency range of 3.5–5 GHz and had an average gain of 2.99 dBi [19]. A horn antenna was combined with a Cylindrical Dielectric Resonator Antenna (CDRA) and used in 5G systems operating in a frequency range of 27.7–32.7 GHz with an average gain of 11.3 dBi [20]. A cone antenna arranged in a dual 1×2 array was used in conjunction with the Complementary Split Ring Resonators (CSRRs) in the VHF/UHF bands operating in the 0.1–0.5 GHz frequency range with an average gain of 7.5 dBi [21].

In the section of microstrip antenna and EBG, the first technique studied was microstrip patch antenna used to determine the moisture content of hevea rubber latex, which was tested at the frequency ranges from 1 GHz, 2 GHz, 3 GHz, 4 GHz, and 5 GHz, and it is found that the 3 GHz range has the lowest humidity error 0.06 [22]. The second technique for microstrip patch antenna using U-shaped patch technique was used to measure the moisture sensor at frequencies of 5.2 GHz and 6.8 GHz, which can measure humidity 10.71%–21.87% with the lowest Mean Relative Error (MRE) 0.55% [23]. The microstrip antenna uses U-shape patch technique to detect salt and sugar by measuring the humidity using frequencies from 3 to 9 GHz. In this moisture determination experimented in the frequency

ranges, the greatest effects on salt and sugar moisture values were 3.4 GHz, 5.8 GHz, 6.2 GHz, and 8.9 GHz. The amount of salt and sugar was then measured at 20 g, 30 g, 40 g, and 50 g. The results showed that efficiencies were 75.44%, 85%, 90%, and 69%, respectively [24]. The microstrip antenna is used to measure the moisture content of paddy in real time, which operates in the frequency band from 3 GHz, and can measure humidity 13.6–27.02%wb. with minimum humidity error 0.17% [25]. A slot-coupled microstrip antenna was used in conjunction with a Partially Reflecting Surface (PRS) 11×11 geometry EBG with the size of $6.6 \times 6.6 \text{ cm}^2$ operating in a frequency range from 9–11 GHz had an average gain of 3.7 dB [26]. A rectangular microstrip antenna with an H-shaped grooving was adopted in X-band with single-layer metasurface for Linear-to-Circular (LP-CP) polarization conversion EBG with a 5×5 layout which operated in a frequency range of 9.5–11.5 GHz and had an average gain of 10 dBic [27]. A rectangular microstrip antenna was implemented in WiMAX and had a gain of 3.55 dBi. This antenna combined a circular EBG with a square reflector arranged in a 6×6 configuration, used a frequency range of 4.93–5.89 GHz, and had an average gain of 12.48 dBi [28].

According to the above, using a waveguide antenna structure and microstrip antenna in combination with an EBG plate has the advantages of increasing the appropriate gain as needed, but it also has disadvantages in terms of complex structure and large size. From the foregoing, this study focuses in a waveguide antenna structure in combination with I-shaped EBG sheets [14–16, 29] due to its simple structure (for measuring moisture content and bulk density of goat manure).

The moisture test data of goat manure was used to calculate the prototype antenna design. The simulation and measurement comparison results of the waveguide antenna with the EBG are shown in Section 2. The test data for moisture content and bulk density of goat manure are discussed in Section 3. The comparison of data between the prototype antenna properties with EBG and the ones from previous studies is in Section 4 and conclusion of the research in Section 5.

2. ANTENNA STRUCTURE DESIGN AND ANTENNA PROPERTIES MEASUREMENT

2.1. Antenna Structure Design

In the antenna design, the moisture content of the goat manure was measured with a frequency probe capable of deep penetration measurement of rectangular waveguide antenna structures and basic antenna [30–32]. Goat manure trays to be measured have thickness ranging from 1–3 cm. The research team compared the two antenna structures to determine the best antenna structure for use in the measurement of moisture content and bulk density as shown in Figure 1(a). It could measure frequencies

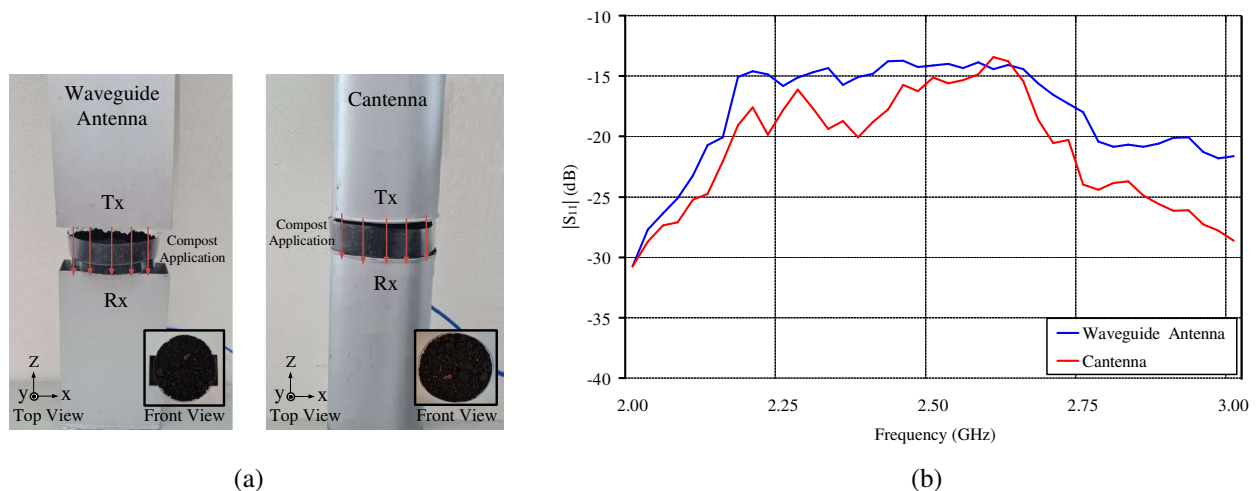


Figure 1. Testing of the two waveguide antennas to measure the moisture content of goat manure at 50%wb.. (a) Images of two waveguide antennas. (b) Simulation of the effect of $|S_{11}|$ (dB) values on measuring the moisture content.

from 2 to 3 GHz and has been checked in practical distances from 1 cm, 3 cm, and 5 cm. The tests showed that the most responsive frequency range was 2.60 GHz at an optimum distance of 3 cm. The moisture content of goat manure was measured at 50%wb. because this affected the frequency band the most as shown in Figure 1(b). In this study, a basic cantenna structure was selected because it transmitted more coverage of the round tray of goat manure than the rectangular waveguide antenna structure. The antenna structure model was designed on a galvanized sheet with thickness value (h_1) = 0.04 cm which can be calculated as in Equations (1)–(7) [30–32]. By the design that uses a CST Microwave Studio simulation program to determine the best parameters of the antenna to be measured $|S_{11}|$ (dB), effective permittivity, VSWR, $Z_{in}(\Omega)$, gain, and radiation pattern, the antenna has dimensions of $5.07 \times 11.61 \text{ cm}^2$ as shown in Figure 2(a) and an impedance bandwidth of 8.46% (2.49–2.71 GHz) as shown in Figure 2(b), which covers the desired frequency range.

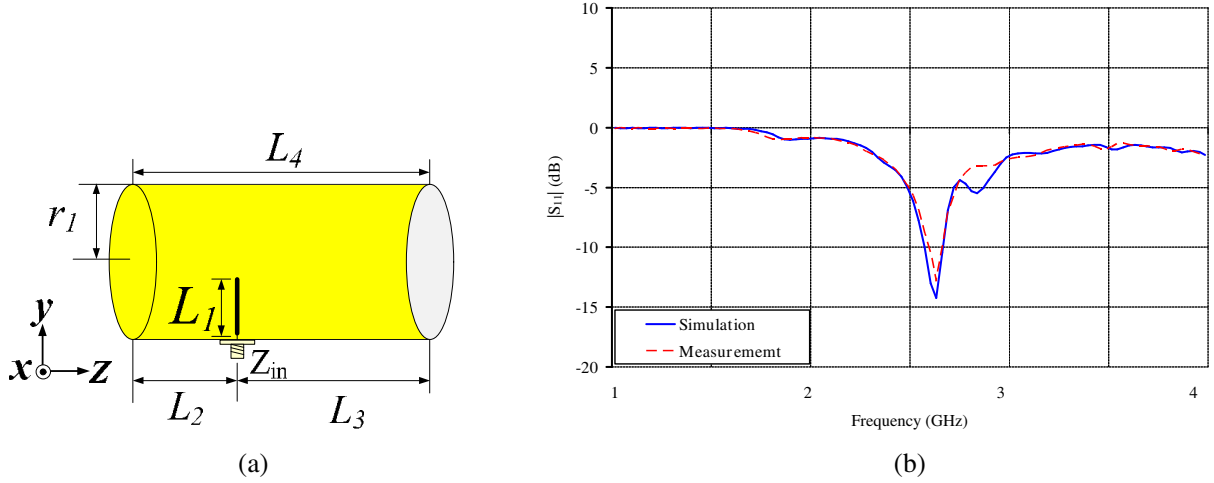


Figure 2. Antenna structure design and comparison between simulation and measurement results. (a) Cantenna. (b) $|S_{11}|$ (dB).

Calculation of cutoff wavelengths (λ_c) is equal to 17.30 cm as in Equation (1).

$$\lambda_c = \frac{c}{f_n} : f_n = \frac{f_r}{1.5} \quad (1)$$

The wavelength in the conductor (λ_g) is equal to 15.48 cm as shown in Equation (2).

$$\lambda_g = \frac{\lambda}{\sqrt{1 - \left(\frac{\lambda}{\lambda_c}\right)^2}} : \lambda = \frac{c}{f_r} \quad (2)$$

The width of the diameter of the circular waveguide antenna (r_1) is 5.07 cm as shown in Equation (3).

$$r_1 = \frac{0.293c}{f_n} \quad (3)$$

The length of the monopole antenna (L_1) is equal to 2.88 cm as in Equation (4).

$$L_1 = \frac{0.25c}{f_r} \quad (4)$$

The distance from the monopole antenna to the end of the spherical waveguide (L_2) is 3.87 cm as shown in Equation (5).

$$L_2 = 0.5\lambda_g \quad (5)$$

The distance from the monopole antenna to the waveguide muzzle (L_3) is 7.74 cm as shown in Equation (6).

$$L_3 = 0.25\lambda_g \quad (6)$$

The length of the conical horn (L_4) is equal to 11.61 cm as in Equation (7).

$$L_4 = 0.75\lambda \quad (7)$$

The test to measure the moisture of goat manure at 2.60 GHz frequency revealed that the signal strength was the lowest at 0.001 uW. In practical applications, there were problems due to the transmitter having a low power about -5 dBm or 100 uV as set according to the standard, which resulted in the receiving sector getting a low power as well. Based on this problem, Woodpile-shaped EBG with Mu-Epsilon Near Zero properties was designed. This type of EBG allowed the wave to propagate through it to increase the gain [33–35]. The antenna was modeled on a polyester mylar film with a thickness of the base material (h_2) = 0.3 cm and a dielectric constant (ϵ_r) = 3.2. The thickness of copper conductor material (t_1) = 0.0297 cm, and the width of the EBG had a wavelength of $0.023\lambda < W_1 < 0.070\lambda$. The distance of (W_1) was adjusted from 0.272 cm, 0.545 cm, and 0.817 cm. From the tuning, it was found that the best value was (W_1) = 0.545 cm and the gap between two EBGs (g_1) = 0.545 cm as shown in Figure 3(a). The range of operating frequency was 3.45% (2.56–2.65 GHz) as shown in Figure 3(b), with a strip line medium ϵ_{SM} , which can be obtained from Equations (8)–(9) [16]

$$\epsilon_{SM} = \epsilon_0 \epsilon_{rh} \left(1 - \frac{k_p^2}{\epsilon_{rh} k_0^2 - k_y^2} \right) : \quad k_0^2 = \frac{\omega}{c} \quad (8)$$

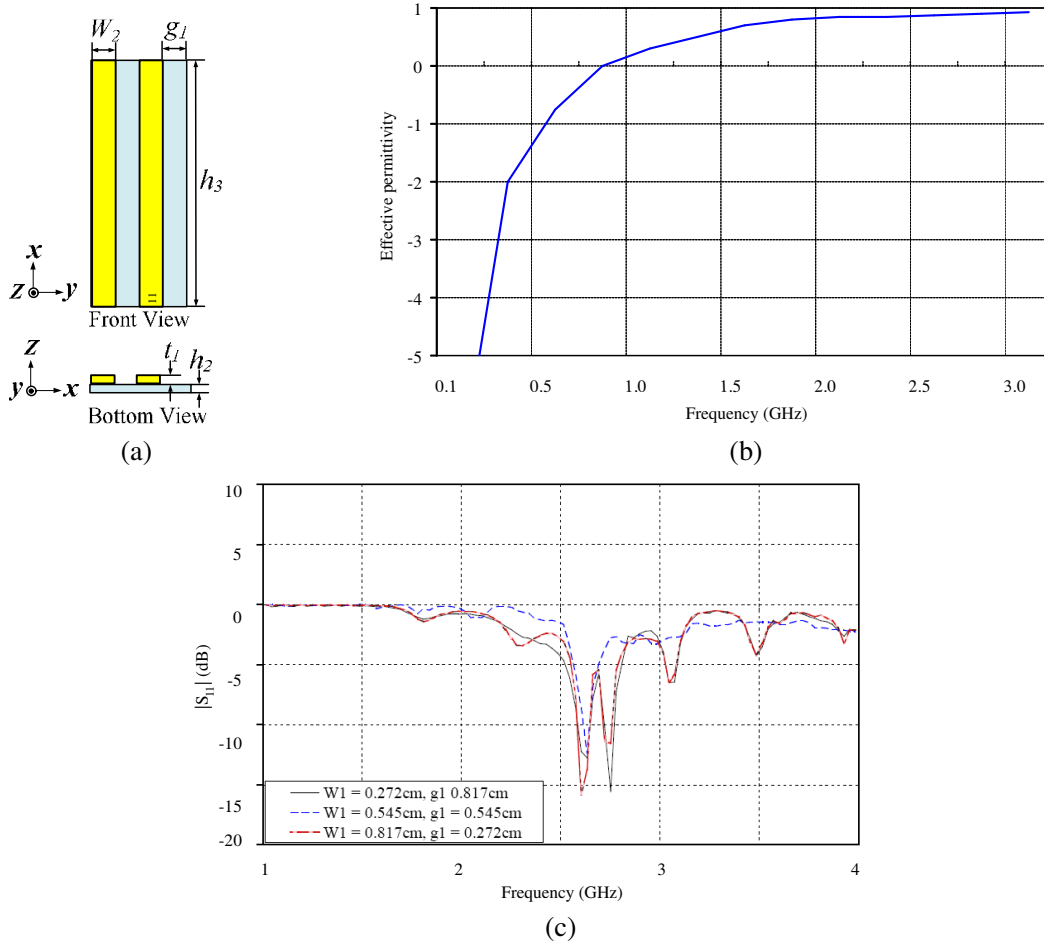


Figure 3. Simulation of the EBG structure. (a) Unit cell of I-shaped EBG. (b) Effective permittivity. (c) Simulation and measurement results $|S_{11}|$ (dB) when the W_1 and g_1 were adjusted.

$$k_p^2 = \frac{2\pi}{(W_1)^2 \left[\ln \left(\frac{W_1}{2\pi t_1} \right) + 0.5275 \right]} \quad (9)$$

ε_{SM} = effective permittivity strip line medium

ε_{rh} = permittivity of the host medium

k_p = plasma frequency

W_1 = the width of EBG (cm)

g_1 = the gap between two EBGs (cm)

t_1 = the thickness of copper conductor material (cm).

The calculation revealed at 2.60 GHz, the effective electrical permittivity of strip line medium of the structure ε_{SM} as shown in Figure 3(c), which allowed wave to propagate through it at 3.45% (2.56–2.65 GHz) with a gain of 9.41 dBi. It is placed at a distance of 0.25λ and has a value $(h_3) = 2.88$ cm. From the above simulation results, a new layout to find the best gain was Transverse Electric (TE) polarization and Transverse Magnetic (TM) polarization as shown in Figure 4(a). The arrangement was done in front of the cantenna [14] with 1×6 units of EBG, by adjusting the distance (h_3) to find the best distance with wavelength values ranging from $0.086\lambda < h_3 < 0.43\lambda$, and the distance is -3 cm to 5 cm, in which the distances of -3 cm and -1 cm are the placement in the waveguide as shown in Figure 4(b). From the adjustment, it was found that the TE arrangement was the most effective. This can be observed from the directional radiation pattern as shown in Figure 5(a). However, the TM arrangement had *forward scattering radiation pattern* in all three directions: top, middle, and bottom, as shown in Figure 5(b). This resulted in a lower gain than TE as shown in Table 1. The TE arrangement resulted in an expansion rate at the distance (h_3) of 3 cm with the gain increasing to 9.47 dBi from 7.89 dBi at a frequency range 4.99% (2.54–2.67 GHz) as shown in Figure 6. The addition of an EBG can optimize the gain of the cantenna structure, by making the directional wave propagation in front of the antenna more distant. The addition of an EBG can enhance the gain efficiency of the cantenna structure, making the wave radiate further in front of the antenna, which is consistent with theory [33–36]. The same frequency band is still used that is 2.60 GHz from the foregoing as displayed in Table 2. The parameters from the best adjustment are shown in Table 3.

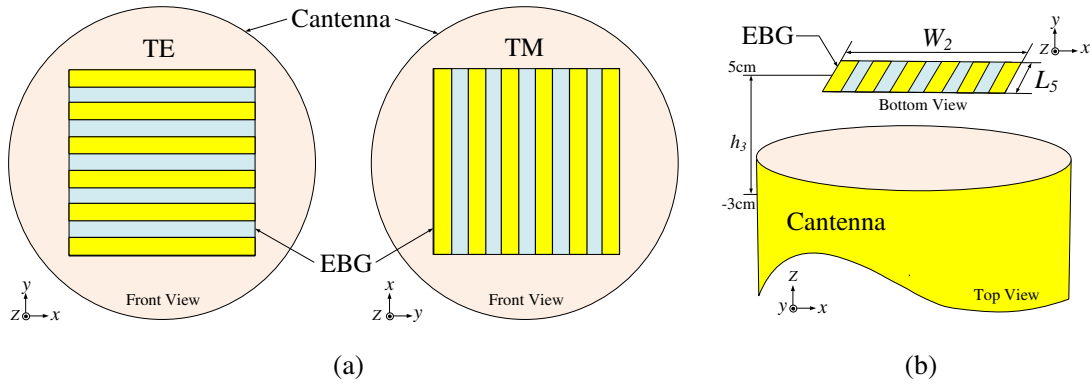


Figure 4. Simulation. (a) TE and TM. (b) Distance between cantenna and EBG.

2.2. Measurement of Antenna Properties

The design of the cantenna structure with the EBG arranged in a planar plane was built as shown in Figures 7(a)–(b). The antenna properties were measured with the Network Analyzer model E5071C as shown in Figure 7(c). The reflection coefficient ($|S_{11}| < -10$ dB), Voltage Standing Wave Ratio (VSWR), impedance (Z_{in}), and gain at the frequency range of 2.60 GHz were measured. From the measurement results to be compared, all 4 as shown in Figure 8 values will be clearly shown as in Table 4, and the comparison of measured and simulated results is shown in Figure 8 and Table 4. The results were similar, and the energy emission pattern was directional, theoretically shown in Figure 9,

Table 1. Distance between cantenna and EBG simulations.

Distance between cantenna and EBG (cm)	Transverse Electric (TE)	Transverse Magnetic (TM)
	Gain (dBi)	Gain (dBi)
−3	8.82	4.91
−1	9.09	4.86
0.1	9.30	4.82
1	9.33	4.25
3	9.47	3.97
5	9.39	3.53

Table 2. Comparison of measured properties of a cantenna in combination with a 2.60 GHz.

Antennas	$ S_{11} $ (dB)	VSWR	Gain (dBi)	$Z_{in}(\Omega)$
Waveguide antenna without EBG	−14.24	1.28 : 1	7.89	52.28-j10.11
Waveguide antenna with EBG at a distance of 3 cm	−12.41	1.46 : 1	9.47	47.84-j23.09

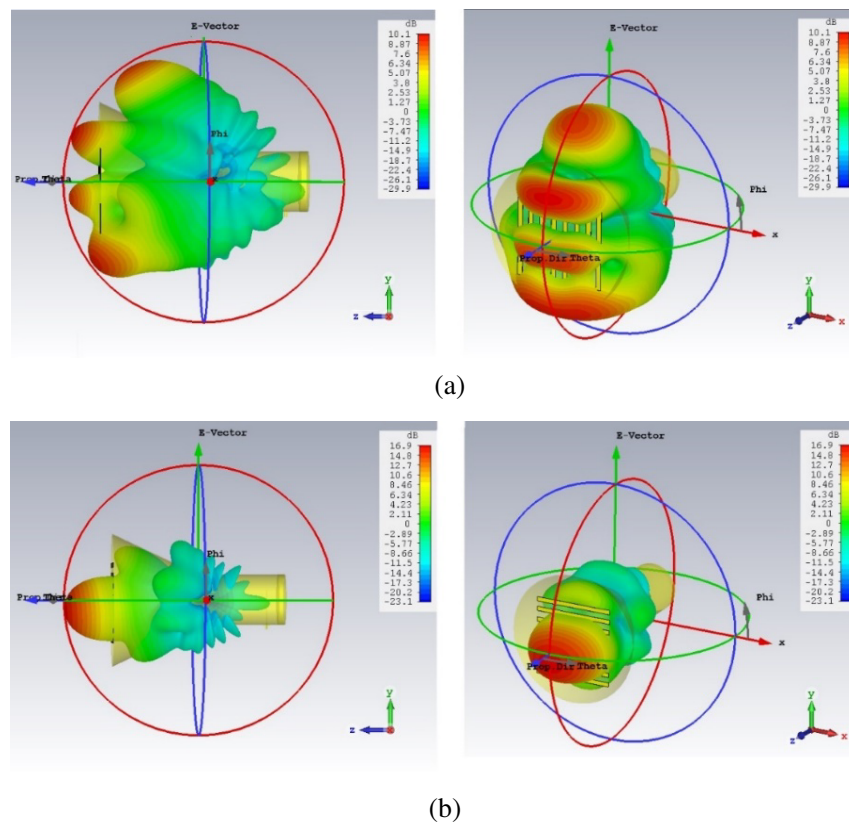
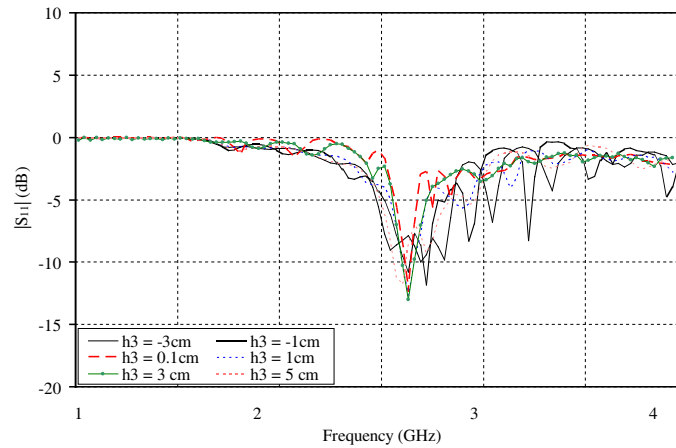
**Figure 5.** The antenna's 3D radiation pattern used in conjunction with an EBG. (a) Placement of EBG in TE layout in the antenna. (b) Placement of EBG in TM layout in the antenna.

Table 3. Values for various variables of the antenna.

Variable	Meaning	Size (cm)
W_1	The width of the EBG	0.545
W_2	The width of the EBG base	6
L_1	The length of the monopole antenna	2.88
L_2	The distance from the monopole antenna to the end of the circular waveguide	3.87
L_3	The distance from the monopole antenna to the spherical waveguide muzzle	7.74
L_4	The length of the spherical waveguide cylinder	11.61
L_5	The length of EBG	6
r_1	The radius of spherical waveguide antenna	5.07
h_1	The length of cantenna	0.04
h_2	The thickness of polyester mylar film base	0.03
h_3	The distance between EBG and cone base	0.1
t_1	Thickness of copper conductor material of EBG	0.0297
g_1	The distance between each EBG	0.545

Table 4. Comparison of measurement properties of waveguide antennas with 2.60 GHz EBG.

Antenna		$ S_{11} $ (dB)	VSWR	Gain (dBi)	Z_{in} (Ω)
Simulation	waveguide antennas	-14.24	1.28 : 1	7.89	52.28-j10.11
	waveguide antennas with EBG	-12.41	1.46 : 1	9.47	47.84-j23.09
Measurement	waveguide antennas	-12.83	1.28 : 1	7.32	48.22-j1.98
	waveguide antennas with EBG	-11.89	1.46 : 1	9.31	53.24-j11.46

**Figure 6.** Simulation of the results of $|S_{11}|$ (dB) from adjusting the value h_3 .

as desired due to its simple structure and easy design [36]. In the antenna operation, a network analyzer transmitter transmits frequency energy to the I-shaped probe. The probe acts as a transducer for the electrical frequency transmitted to the air in the cantenna as shown in Figure 2(a). The cantenna acts as a frequency radiation controller to direct the wave energy from the probe forward to the EBG with its

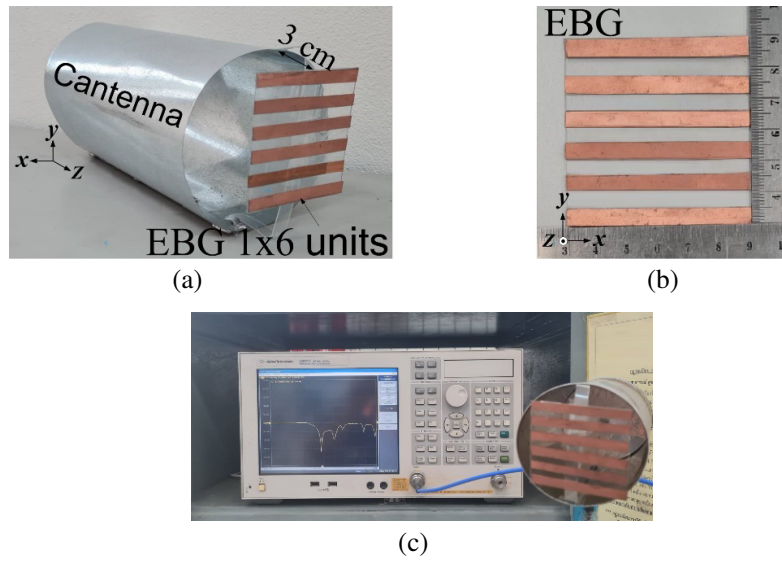


Figure 7. Cantenna with EBG at the distance of 3 cm. (a) Cantenna with EBG. (b) The various shaped woodpile EBG. (c) Measurement method.

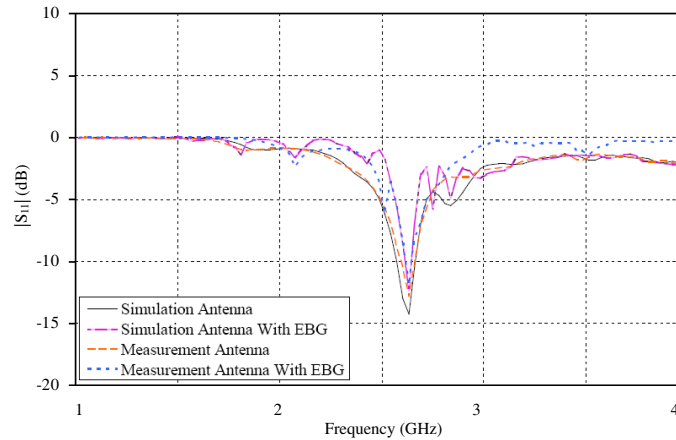


Figure 8. Comparison of simulation results and measurement results $|S_{11}|$ (dB).

penetrating properties. This makes the spectrum power even more amplified to 9.31 dBi from 7.32 dBi as shown in Figure 7(a).

3. SPECTRUM TESTING MEASUREMENT OF THE MOISTURE CONTENT IN GOAT MANURE

Goat manure and straw were fermented for 3 months using aerobic fermentation as shown in Figure 10. The results were then measured with a LiteVNA model 64 transmitter with the signal strength set at -10 dBm or 0.1 mW as shown in Figure 10. The transmitter used to measure signal strength is set to -10 dBm or 0.1 mW as show in Figure 10. Test showed that moisture determination of goat manure with size 4×3 cm² using microwave resonance with the EBG cantenna can be measured from 1–100%wb. The BD values ranged from 300 to 1000 kg/m³ as shown in Figure 11 whereby the moisture content can be calculated as Equation (10) [37] and averaged from 300–1000 kg/m³ with the average power of 0.0001–0.07 mW as shown in Figure 12. The bulk density can be calculated as shown in Equation (11) [38].

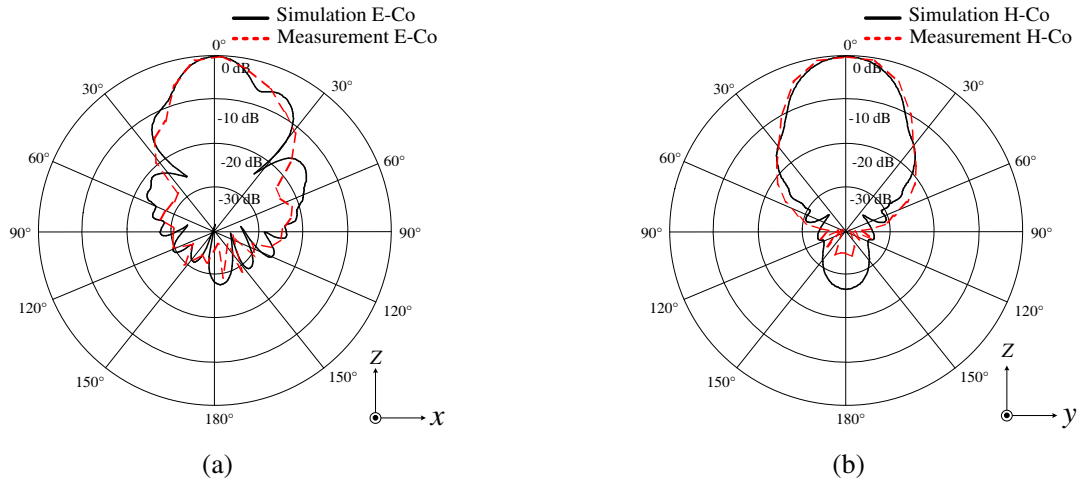


Figure 9. Comparison of simulation with measurement results of electric and magnetic field emission patterns. (a) Electric field. (b) Magnetic field.

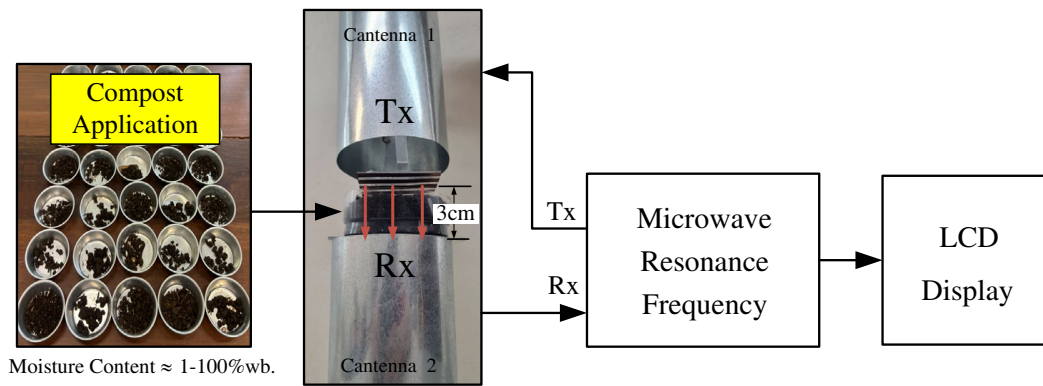


Figure 10. Measurement of moisture content and bulk density of goat manure by antenna.

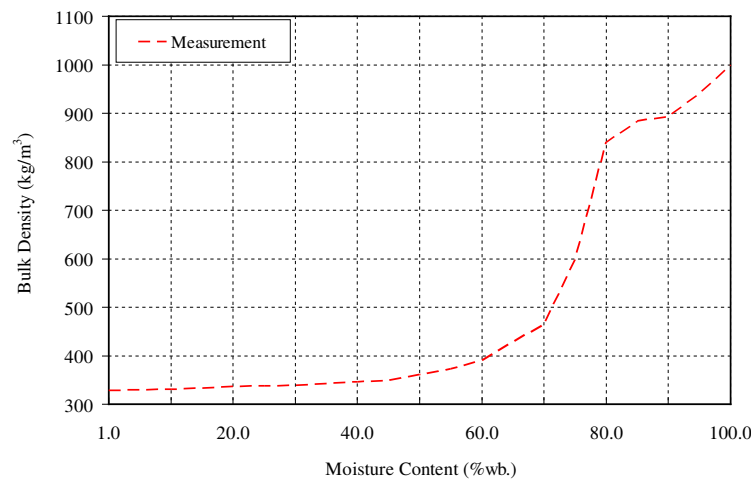


Figure 11. The moisture content measurement result of goat manure.

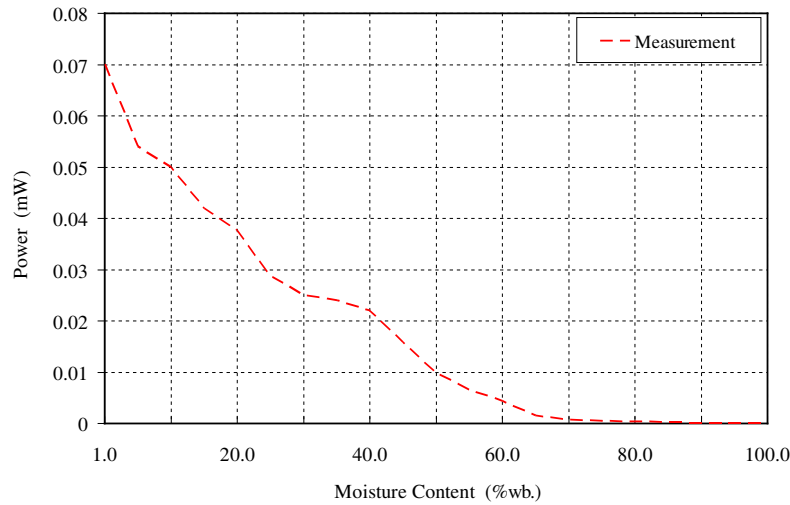


Figure 12. The bulk density measurement result of goat manure.

The Moisture Content (MC) is calculated as shown in Equation (10).

$$MC = \frac{SWBB - SWAB}{SWBB} \times 100 \quad (10)$$

The Bulk Density (BD) is calculated as shown in Equation (11).

$$BD = \frac{SW}{V} \quad (11)$$

MC = Moisture Content (%wb.)

BD = Bulk Density (kg/m³)

SWBB = Sample Weight Before Baking (g)

SWAB = Sample Weight After Baking (g)

SW = Sample Weight (kg)

V = Volume (g/m³)

wb. = Wet basis (wb.).

Wet basis is the moisture value that is often used in commercial applications. It is a value used to indicate the humidity in general in everyday life usually expressed as a percentage.

Table 5. Efficiency comparison of rectenna.

Reference	Frequency (GHz)	Shaped EBG	Substrate EBG		Thickness (cm)	Gain (dBi)
			Substrate	Size (cm ³)		
[9]	10	Woodpile	Aluminum	45 × 0.19	49.5	25.60
[10]	1, 1.3	Woodpile	Aluminum	40 × 40 × 7.62	4.77	15.61, 14.46
[14]	0.60–3	Woodpile	Aluminum	15.12 × 0.16	49.5	25.34
[15]	0.65–5	Wire	Copper	21.88 × 0.18	0	19.70
[16]	10	Wire	Copper	6 × 6 × 0.85	0	20.90
[19]	3.5–5	FSS grid	Copper	23.95 × 23.95 × 0.25	0	2.99
Proposed	2.56–2.65	Woodpile	Copper	6 × 6 × 0.0597	3	9.31

4. COMPARISON BETWEEN THE PROTOTYPE ANTENNA AND ANTENNAS FROM PREVIOUS RESEARCH

The comparison, as shown in Table 5, demonstrated that the compared study had advantages in terms of the size of the structure of the EBG. The distance from the dipole antenna to the EBG in all works was small, except [9] and [14] which both had a distance of 49.5 cm. The gain was greater than the other compared works, except [19] because it is designed for application in goat manure moisture content and bulk density monitoring, whose cantenna and the prototype woodpile shape also had the advantage of being simple in design. The thin structure was lighter due to the use of polyester mylar base plate than the antennas from other researches.

5. CONCLUSION

In the study of the structure of the cantenna with the 1×6 units woodpile shape EBG was used to measure moisture and density of goat manure. The results were measured at the best humidity response frequency band of 2.60 GHz. Transmission distance between cantenna Tx/Rx is 3 cm. The results were repeated 10 times per experiment. The antenna can measure moisture content 1–100%wb. with an average bulk density from 300 to 1000 kg/m³. It has an average power from 0.0001–0.5 mW. The measurement of the antenna properties has the operating frequency range 3.45% (2.56–2.65 GHz) and impedance 53.24–j11.46 Ω . The EBG has directional emission characteristics with a gain of 9.31 dBi, arranged in transverse electric (TE) and placed parallel to the end of the cantenna. The efficiency of moisture determination is 98.33%. From the research mentioned above, there are advantages in the structure of the cantenna with the EBG, which is a simple design, a few adjusting points, not complicated, and cheap. This research can be developed to apply to agricultural manures of Thailand such as bat manure, chicken manure, pig manure, buffalo manure, and cow manure.

ACKNOWLEDGMENT

We would like to thank the Department of Electronic and Telecommunications Engineering, Faculty of Engineering, Rajamangala University of Technology Phra Nakhon and Department of Telecommunications Engineering, Faculty of Engineering and Technology, Rajamangala University of Technology Isan to support the research successfully.

REFERENCES

1. Zhang, J., Y. Ying, and X. Yao, "Effects of turning frequency on the nutrients of *Camellia oleifera* shell co-compost with goat dung and evaluation of co-compost maturity," *Plos One*, Vol. 14, No. 9, e0222841, 2019.
2. Situmeang, Y. P., I. D. N. Sudita, and M. Suarta, "Manure utilization from cows, goats, and chickens as compost, biochar, and poschar in increasing the red chili yield," *International Journal on Advanced Science, Engineering and Information Technology*, Vol. 9, No. 6, 2088–2095, 2019.
3. Noreen, N. A. Y. A. R. A., N. A. D. I. A. Ramzan, Z. A. H. I. D. A. Perveen, and S. A. L. E. E. M. Shahzad, "A comparative study of cow dung compost, goat pellets, poultry waste manure and plant debris for thermophilic, thermotolerant and mesophilic microflora with some new reports from Pakistan," *Pak. J. Bot*, Vol. 51, No. 3, 1155–1159, 2019.
4. Ani, K. A., C. M. Agu, C. Esonye, and M. C. Menkiti, "Investigations on the characterizations, optimization and effectiveness of goat manure compost in crude oil biodegradation," *Current Research in Green and Sustainable Chemistry*, Vol. 4, 100120, 2021.
5. Ren, X., Z. Wang, M. Zhao, J. Xie, Z. Zhang, F. Yang, and Y. Ding, "Role of selenite on the nitrogen conservation and greenhouse gases mitigation during the goat manure composting process," *Science of the Total Environment*, 155799, 2022.
6. Meyer, D., P. Price, and B. Karle, "Solid manure moisture content determination-microwave method for exported solid manures," *California Dairy Quality Assurance Program*, 2008.

7. Pankaj, P., P. Kaur, and K. Singh Mann, "Frequency, temperature and moisture dependent dielectric properties of chicken manure relevant to radio frequency/microwave drying," *Poultry Science Journal*, Vol. 9, No. 2, 187–195, 2021.
8. Luo, T., Y. Wang, and P. Pandey, "The removal of moisture and antibiotic resistance genes in dairy manure by microwave treatment," *Environmental Science and Pollution Research*, Vol. 28, No. 6, 6675–6683, 2021.
9. Kampeephath, S., P. Krachodnok, and R. Wongsan, "Efficiency improvement for conventional rectangular horn antenna by using EBG technique," *International Journal of Electrical, Computer, Energetic, Electronic and Communication Engineering*, Vol. 8, No. 7, 1038–1043, 2014.
10. Wongsan, R. and P. Khamsalee, "Hybrid metamaterial structure for asymmetric horn of secondary radar system," *2019 7th International Electrical Engineering Congress (iEECON)*, 1–4, IEEE, March 2019.
11. Karami-Raviz, A. and S. E. Hosseini, "A novel horn antenna with a bed of nails with high gain and low side lobes," *2020 28th Iranian Conference on Electrical Engineering (ICEE)*, 1–4, IEEE, August 2020.
12. Sifat, S. M., S. I. Shams, and A. A. Kishk, "Ka-band integrated multilayer pyramidal horn antenna excited by substrate integrated gap waveguide," *IEEE Transactions on Antennas and Propagation*, Vol. 70, No. 6, 4842–4847, 2021.
13. Yoshida, K., N. Kashiyama, M. Kanemoto, S. Umemoto, H. Nishikawa, A. Tanaka, and T. Douseki, "2.45-GHz wireless power transmitter with dual-polarization-switching cantenna for LED accessories," *2019 IEEE Wireless Power Transfer Conference (WPTC)*, 371–374, IEEE, June 2019.
14. Wongsan, R., P. Krachodnok, S. Kampeephath, and P. Kamphikul, "Gain enhancement for conventional circular horn antenna by using EBG technique," *2015 12th International Conference on Electrical Engineering/Electronics, Computer, Telecommunications and Information Technology (ECTI-CON)*, 1–4, IEEE, June 2015.
15. Wongsan, R., P. Duangtang, and P. Mesawad, "Dimension reduction of conical horn antennas by adding structure of metamaterial," *2015 IEEE Asia Pacific Conference on Wireless and Mobile (APWiMob)*, 214–217, IEEE, August 2015.
16. Duangtang, P., P. Mesawad, and R. Wongsan, "Creating a gain enhancement technique for a conical horn antenna by adding a wire medium structure at the aperture," *Journal of Electromagnetic Engineering and Science*, Vol. 16, No. 2, 134–142, 2016.
17. Xu, Y. X. and Y. B. Tian, "Optimal design of conical horn antenna based on GP model with coarse mesh," *Iranian Journal of Science and Technology, Transactions of Electrical Engineering*, Vol. 43, No. 4, 717–724, 2019.
18. Ridho, S., C. Apriono, F. Y. Zulkifli, and E. T. Rahardjo, "Design of corrugated horn antenna with wire medium addition as parabolic feeder for Ku-band very small aperture terminal (VSAT) application," *2020 International Conference on Radar, Antenna, Microwave, Electronics, and Telecommunications (ICRAMET)*, 163–166, IEEE, November 2020.
19. Dhandhukia, H. and D. Pujara, "Fabry-Perot horn antenna with improved gain," *2020 IEEE International Symposium on Antennas and Propagation and North American Radio Science Meeting*, 1973–1974, IEEE, July 2020.
20. Baldazzi, E., A. Al-Rawi, R. Cicchetti, A. B. Smolders, O. Testa, C. D. J. van Coevorden Moreno, and D. Caratelli, "A high-gain dielectric resonator antenna with plastic-based conical horn for millimeter-wave applications," *IEEE Antennas and Wireless Propagation Letters*, Vol. 19, No. 6, 949–953, 2020.
21. Ni, C., J. Jiang, W. J. Wu, L. Zhao, and Z. Fan, "Decoupling method based on complementary split ring resonator (CSRR) for two cone shipborne antennas," *IEEE Access*, Vol. 9, 167845–167854, 2021.
22. Yahaya, N., Z. Abbas, M. A. Ismail, and B. M. Ali, "Determination of moisture content of hevea rubber latex using a microstrip patch antenna," *PIERS Proceedings*, 1290–1293, Kuala Lumpur, Malaysia, March 27–30, 2012.

23. Jain, S., P. K. Mishra, V. V. Thakare, and J. Mishra, "Microstrip moisture sensor based on microstrip patch antenna," *Progress In Electromagnetics Research M*, Vol. 76, 177–185, 2018.
24. Jain, S., "Early detection of salt and sugar by microstrip moisture sensor based on direct transmission method," *Wireless Personal Communications*, Vol. 122, No. 1, 593–601, 2022.
25. Liu, J., S. Qiu, and Z. Wei, "Real-time measurement of moisture content of paddy rice based on microstrip microwave sensor assisted by machine learning strategies," *Chemosensors*, Vol. 10, No. 10, 376, 2022.
26. Li, Z., Y. Wang, and X. Qu, "Design of high gain broadband antenna based on Fabry-Perot resonator," *Proceedings of the 3rd International Conference on Vision, Image and Signal Processing*, 1–5, August 2019.
27. Swain, R., A. Chatterjee, S. Nanda, and R. K. Mishra, "A linear-to-circular polarization conversion metasurface based wideband aperture coupled antenna," *Journal of Electrical Engineering & Technology*, Vol. 15, No. 3, 1293–1299, 2020.
28. Srinivas, G. and D. Vakula, "High gain and wide band antenna based on FSS and RIS configuration," *Radioengineering*, Vol. 30, No. 1, 96–103, 2021.
29. Li, Y. L. and K. M. Luk, "Dual circular polarizations generated by self-polarizing Fabry-Pérot cavity antenna with loaded polarizer," *IEEE Transactions on Antennas and Propagation*, Vol. 69, No. 12, 8890–8895, 2021.
30. Muñoz Jaramillo, F. P., "Departamento de eléctrica, electrónica y telecomunicaciones," Doctoral dissertation, Universidad De Las Fuerzas Armadas, 2020.
31. Santosa, S. P. and A. Nurdianto, "Rancang bangun antenna kaleng di frekuensi 2.4 GHz untuk memperkuat sinyal WIFI," *Seminar Nasional Teknologi*, Vol. 1, No. 1, 574–580, May 2018.
32. Pahrurrozi, P., C. M. O. Muvianto, and S. Ariessaputra, "Desain modifikasi cantenna untuk optimasi feed antenna grid 2.4 GHz," *Jurnal Bakti Nusa*, Vol. 1, 49–57, 2020.
33. Bakhtiari, A., "Investigation of enhanced gain miniaturized patch antenna using near zero index metamaterial structure characteristics," *IETE Journal of Research*, Vol. 68, No. 2, 1312–1319, 2022.
34. Fhafhiem, N., P. Krachodnok, and R. Wongsan, "Curved strip dipole antenna on EBG reflector plane for RFID applications," *WSEAS Transactions on Communications*, Vol. 9, No. 6, 374–383, 2010.
35. Naktong, W. and N. Wattikornsirikul, "Dipole antenna with 18×5 square electromagnetic band gap for applications used in monitoring children trapped in cars," *Progress In Electromagnetics Research M*, Vol. 112, 163–176, 2022.
36. Balanis, C. A., *Antenna Theory and Design*, John Wiley & Sons, NY, USA, 1997.
37. Horwitz, W. and G. W. Latimer, *Official Methods of Analysis*, 18th Edition, AOAC International, USA, 2005.
38. ISO 3944, "Fertilizers — Determination of bulk density (loose)," International Standard, 1992.